submitted to Phys. Rev. B

Statistical properties of level widths and conductance peaks in a quantum dot

E. R. Mucciolo[†], V. N. Prigodin[‡], and B. L. Altshuler[†]
[†]*Department of Physics, Massachusetts Institute of Technology, Cambridge, Massachusetts 02139*
and
[‡]*Max-Planck-Institut für Festkörperforschung, Postfach 80 06 65, D-70506 Stuttgart, Germany*
(June 10, 1994)

arXiv:cond-mat/9406048v1 10 Jun 1994

Abstract

We study the statistics of level widths of a quantum dot with extended contacts in the absence of time-reversal symmetry. The widths are determined by the amplitude of the wavefunction averaged over the contact area. The distribution function of level widths for a two-point contact is evaluated exactly. The distribution resembles closely the result obtained when the wavefunction fluctuates independently at each point, but differs from the one-point case. Analytical calculations and numerical simulations show that the distribution for many-point contacts has a power-law behavior at small level widths. The exponent is given by the number of points in the lead and diverges in the continuous limit. The distribution of level widths is used to determine the distribution of conductance peaks in the resonance regime. At intermediate temperatures, we find that the distribution tends to normal and fluctuations in the height of the peaks are suppressed as the lead size is increased.

73.40.Gk, 73.20.Dx, 05.45.+b

Typeset using REVTEX

I. INTRODUCTION

Usually any measurement of conductance in a metallic system assumes at least two attached leads. The existence of these leads connecting the system to reservoirs broadens the electronic energy levels. For a macroscopic sample, the width of an energy level is typically much larger than the distance between neighboring levels. As a result, one observes a smooth dependence of the conductance on the Fermi energy.

Recently, the advances in nanometer technology have made possible the fabrication of very small semiconductor devices, known generically as quantum dots,[1–3] where one has a fixed number of conduction electrons confined into an island. In these systems, one can narrow the level width by reducing either the size of the leads or their transmittance. In the first case it is customary to speak about channels: If we consider an ideal lead as a wave guide with a given cross section, we can associate a channel to each state due to transverse quantization. The number of channels is approximately the area, in units of electron wavelength, of the contact between lead and dot and each channel is characterized by its transmittance.

The conductance of a system can be calculated through the well-known Landauer-Büttiker formula.[4,5] Following this approach, the distribution of conductances of a quantum dot has been evaluated for two distinct cases: for weakly coupled, pointlike, leads[6] of a closed system, and for leads with any number of channels attached to a ballistic cavity.[7,8]

Here we will consider the situation at low transmittance, when leads behave as tunnel contacts. In this case, each electron eigenstate corresponds to a peak in the Fermi energy (gate voltage) dependence of the conductance.[2,3] This allows one to make a real spectroscopy of electrons in quantum dots. The height of each peak is determined by the probabilities of tunneling through the leads, as well as by the amplitude of the wavefunction near the contacts. The later means that these heights are randomly distributed. The distribution function of the peaks has been determined for the case of pointlike contacts in Refs. 6,9, and 10. In this paper we will deduce the distribution considering leads of arbitrary size.

We begin by studying the statistics of level widths, which is connected to the fluctuations of conductance peaks through the Landauer-Büttiker formula. The supersymmetry technique and the nonlinear σ model[11,12] provide the framework for the exact calculation of the distribution of level widths for leads with two-point contact. The distribution differs drastically from the single-point case, but we find that inclusion of correlation between the wavefunction fluctuations at the two points in the lead does not significantly alter the overall form of the distribution of level widths. This analytical result is confirmed through numerical simulations of a quantum dot. The exact distribution of conductance peaks is also evaluated for two-point leads and we find that it deviates from the single-point distribution mainly for small peak heights, where it shows a linear dependence.

For leads with many-point contacts we do not know of any method which enables a general evaluation of the distribution function of level widths. Thus we assume that the wavefunction at each point fluctuates independently and proceed to calculate the total distribution. By comparing numerical with analytical results, we show that this approximation yields a good qualitative understanding of the large-lead limit, since correlations do not effect the behavior of the distribution very strongly.

An important use of quantum dots is found in the study of chaos.[13–18] Because one can

obtain extremely clean samples and shape them into different forms, it is now possible to fabricate the so-called quantum billiards, where one has a unique chance to study quantum and semiclassical physics.[13,19] Although the supersymmetry method assumes averaging over disorder, one can conjecture on very firm grounds (the ergodic hypothesis) that it applies quite generally to quantum chaos problems. Therefore, we expect that our results should be able to describe any system where the underlying dynamics is chaotic, regardless as to whether it is diffusive or ballistic

The organization of this paper goes as follows. In Sec. II we describe the model used and the basic concepts related to conductance peaks and level widths. The way the numerical simulations were done is explained in Sec. III. Some of the results found in Ref. 6, which initially motivated the present work, are reviewed in Sec. IV. The case of two-point leads is treated exactly in Sec. V and the case of many-point leads, under the approximation of independent point fluctuations, is left to Sec. VI. Finally, in Sec. VII we draw our conclusions and point out some experimental consequences of our work.

II. FORMULATION OF THE PROBLEM

The electronic system we consider is formed by noninteracting spinless fermions confined to a small region through some strong confining potential. The system is probed by two leads, described by discrete sets of points, which are weakly coupled to the system. More precisely, we have the Hamiltonian[6,20]

$$H = -\frac{\nabla^2}{2m} + U(r) + \frac{i}{2\pi\mathcal{N}} \left[\alpha_1 \sum_{r\in A_1} \delta(r-r_1) + \alpha_2 \sum_{r\in A_2} \delta(r-r_2) \right] , \tag{1}$$

where $U(r)$ is the potential (containing the effect of random impurities and confining walls) and $\mathcal{N} = 1/(V\Delta)$ is the mean density of states, with V denoting the total volume and Δ the average level spacing. The term inside the brackets represents the contact leads, denoted by $A_{1,2}$, and $\alpha_{1,2}$ are the dimensionless coupling parameters.

In a situation characteristic of scattering experiments, when $\alpha_{1,2} \gg 1$ and the leads are open, the number of channels is equal to the number of wavelengths which fit into the lead cross section. As we shall demonstrate, for the weakly coupled leads of a *closed* quantum dot, the distinction between pointlike (single channel) and multichannel leads is more subtle and deserves a careful analysis.

When tunneling through the leads in totally suppressed ($\alpha_{1,2} = 0$) the energy levels have zero intrinsic width. The levels will gain a small but finite width if the coupling to the leads is made very weak, i.e., if $0 < \alpha_{1,2} \ll 1$. As one can show by first order perturbation theory, the broadening will be caused by local fluctuations of the electron wavefunction in the regions of contact with the leads. Calling the total level width Γ_ν, we have

$$\Gamma_\nu = \gamma_{\nu,1} + \gamma_{\nu,2} , \tag{2}$$

with the partial level widths given by

$$\gamma_{\nu,i} = \alpha_i \left(\frac{V\Delta}{\pi} \right) \sum_{r\in A_i} |\psi_\nu(r)|^2 \qquad (i = 1, 2) , \tag{3}$$

where ψ_ν is a single-particle eigenfunction of the Hamiltonian in Eq. (1) for $\alpha_{1,2} = 0$.

The knowledge of the statistical properties of γ_i is crucial to describe some important and measurable effects in quantum dots. From the distribution of level widths we can extract the distribution of conductance peaks in the resonance regime. It is rather simple to understand why: Let us assume that the conductance at a given energy E can be evaluated through the Landauer-Büttiker formula,[4,5]

$$G(E) = \frac{2e^2}{h} \frac{\alpha_1 \alpha_2}{(\pi \mathcal{N})^2} \sum_{r_1 \in A_1} \sum_{r_2 \in A_2} \left| \sum_\nu \frac{\psi_\nu^*(r_1)\psi_\nu(r_2)}{E - \varepsilon_\nu + i\Gamma_\nu/2} \right|^2 , \tag{4}$$

where ε_ν is the eigenvalue associated with the eigenfunction ψ_ν. In the resonance regime ($\gamma, T \ll \Delta$), only the eigenstate whose energy is the closest to E significantly contributes to the conductance. $G(E)$ is very small when E is between adjacent energy levels, and grows rapidly when $E \to \varepsilon_\nu$. Therefore, at a peak of the conductance, we have

$$G_\nu = \frac{2e^2}{h} \frac{4\alpha_1 \alpha_2}{(\pi \mathcal{N} \Gamma_\nu)^2} \sum_{r_1 \in A_1} \sum_{r_2 \in A_2} |\psi_\nu(r_1)|^2 |\psi_\nu(r_2)|^2 . \tag{5}$$

Using the last equation, plus Eqs. (2) and (3), we obtain the Breit-Wigner formula

$$G_\nu = \frac{2e^2}{h} \frac{4\gamma_{\nu,1}\gamma_{\nu,2}}{(\gamma_{\nu,1} + \gamma_{\nu,2})^2} , \tag{6}$$

which is correct at zero temperature, or when $T \ll \alpha_{1,2}\Delta$. In order to describe a wider range of temperatures, we have to use instead the well-known relation

$$G_\nu = \frac{2e^2}{h} \int \frac{d\epsilon}{4T} \, \frac{\gamma_{\nu,1}\gamma_{\nu,2}}{\epsilon^2 + (\gamma_{\nu,1} + \gamma_{\nu,2})^2/4} \cosh^{-2}\left(\frac{\epsilon}{2T}\right) . \tag{7}$$

Let N be the number of points in each lead. When the leads are placed very far apart, the connection between the distribution of level widths, $P_N(\gamma_{\nu,i})$, and the distribution of conductance peaks, $R_N(g_m)$, is given by the convolution

$$R_N(g_m) = \int_0^\infty d\gamma_{\nu,1} P_N(\gamma_{\nu,1}) \int_0^\infty d\gamma_{\nu,2} P_N(\gamma_{\nu,2}) \; \delta\left(g_m - G_\nu h/2e^2\right) . \tag{8}$$

From Eq. (7) we can extract another limit, which occurs when the temperature exceeds the intrinsic energy level width, $T \gg \alpha_{1,2}\Delta$, but is still low enough so that there are well-resolved resonance peaks ($T \ll \Delta$). In fact, this intermediate regime is typical of some experiments[14] and is described by the Hauser-Feshbach formula

$$G_\nu = \frac{2e^2}{h} \left(\frac{\pi}{2T}\right) \frac{\gamma_{\nu,1}\gamma_{\nu,2}}{\gamma_{\nu,1} + \gamma_{\nu,2}} . \tag{9}$$

In practice, one can generate many peaks in the conductance by varying the energy E (i.e., by sweeping the gate voltage in the quantum dot), or, else, by varying some external parameter, say, an applied magnetic field. Similarly, in numerical calculations one can apply a Aharonov-Bohm flux ϕ to the system, and then generate a family of curves $\varepsilon_\nu(\phi)$, which yields a random sequence of conductance peaks, $G_\nu(\phi)$. As long as the system is ergodic, all these procedures are equivalent to the construction of an ensemble of different realizations of disorder (in the case of a diffusive regime) or boundaries (if the regime is ballistic).

III. NUMERICAL SIMULATION

Before we move to the analytical calculations, let us describe the numerical simulation of a disordered quantum dot which we used to illustrate the main points of our work. The numerical results will be shown along the discussion of the analytical ones. Our motivation was to obtain the histogram $P_N(\gamma)$ as a function of the separation between the points within the lead. We used a two-dimensional Anderson model of noninteracting spinless electrons with nearest-neighbor hopping and diagonal disorder, i.e., the Hamiltonian

$$H_A = -\sum_{\langle i,j \rangle} (c_i^\dagger c_j + c_j^\dagger c_i) + \sum_{i=1}^{N} w_i \; c_i^\dagger c_i \; , \tag{10}$$

with w_i uniformly distributed in the interval $[-W/2 \; , W/2]$. We restricted our calculations to only one realization of $\{w_i\}$; hence, no average over disorder was performed. On the other hand, we imposed quasiperiodic boundary conditions to the electrons by making the geometry toroidal and introducing Aharonov-Bohm phases in the hops,

$$c_i^\dagger c_j \longrightarrow c_i^\dagger c_j e^{-i\phi_{ij}} \; , \tag{11}$$

where ϕ_{ij} assumes one of two values, ϕ_x or ϕ_y, depending on whether the hop occurs along the x or y axis, respectively. By varying ϕ_x and ϕ_y within the interval $(0, \pi)$ we obtained a large set of states, thus creating the statistical ensemble needed to construct the histograms.

For a given set of phases ϕ_x and ϕ_y the Hamiltonian was diagonalized through standard procedures and all eigenstates obtained. The leads were then chosen as sets of sites placed throughout the grid, such that we could probe the density fluctuations at different regions of the dot. Notice that the leads were passive objects, which did not affect the eigenstates.

Briefly, we mention the existence of a technical complication, intrinsic to simulations of quasiperiodic systems, which is the crossover with respect to time-reversal breaking. The threshold for breaking time-reversal symmetry with Aharonov-Bohm fluxes is proportional to the conductance of the system.[21] If the disorder is too strong or the system too small, a complete time-reversal symmetry breaking may never be achieved due to the periodic nature of fluxes. As a result, in order to fall into the class of the unitary ensemble and be able to compare the simulations with the calculations to follow, we needed to work with a large grid (32×23) and keep the disorder very low. The system was then maintained marginally diffusive ($W \approx 1$).

IV. POINTLIKE LEADS

We will consider first the simple case of pointlike leads, namely, when the typical size of the contact is smaller than the area λ^{d-1}, where λ is the electron wavelength. In the lattice version of the problem, this certainly happens when the lead consists of a single site. For a chaotic system with broken time-reversal symmetry, the amplitude $v = V|\psi_\nu(r)|^2$ fluctuates according to an exponential distribution. This result follows from the assumption that the components of the eigenfunction are not correlated among themselves and are uniformly distributed.[22] Therefore, by connecting v to the level width γ_i [see Eq. (3)] we can write

$$P_1(\gamma_i) = \left(\frac{\pi}{\alpha_i \Delta}\right) \exp\left(-\frac{\pi \gamma_i}{\alpha_i \Delta}\right) \ . \tag{12}$$

(To simplify the notation, we will hereafter drop the eigenstate label.) In Fig. 1 we have plotted $P_1(\gamma_i)$ obtained from our numerical simulation against Eq. (12) for two different regions of the spectrum. The states around the bottom of the band used in the evaluation of the level width distribution were checked to be extended over the entire grid.

If the distance between the leads A_1 and A_2 is much larger than the electron wavelength λ (so that the wavefunction fluctuations at r_1 and r_2 are independent), we can use Eq. (6) or Eq. (9), together with Eqs. (8) and (12), to evaluate analytically the distribution of conductance peaks for single-point leads, $R_1(g_m)$. This calculation has been recently done in the literature.[6,9] In Ref. 9 the authors found an expression for the conductance distribution at intermediate temperatures not only for single-channel leads, but for multichannel ones as well. Their derivation, based on random matrix theory, enabled them to consider the case of time-reversal symmetry, although they were constrained to treat only the case of independent channels. In addition, for simplicity, they treated only the situation of symmetric leads. A similar work is found in Ref. 10, where the authors have also studied the effect of chaotic and regular dynamics in the distribution of conductance peaks.

On the other hand, the authors in Ref. 6 performed their analysis exclusively for the case of broken time-reversal symmetry and pointlike leads, but took into account a possible asymmetry between the leads. Since we shall extend their work, we will display and comment on some of their results. For $T \ll \alpha_{1,2}\Delta$ they obtained the following distribution

$$R_1(g_m) = \frac{\theta(1-g_m)}{2\sqrt{1-g_m}} \frac{[1+(2-g_m)(a^2-1)]}{[1+g_m(a^2-1)]^2} \ , \tag{13}$$

where the asymmetry parameter a is given by

$$a = \frac{1}{2}\left(\sqrt{\frac{\alpha_1}{\alpha_2}} + \sqrt{\frac{\alpha_2}{\alpha_1}}\right) \ . \tag{14}$$

Notice that, according to Eq. (14), for $a = 1$ (symmetric leads), the most probable value of g_m is 1. However, for $a > 1$ the distribution begins shifting to lower values of g_m. For $a \gg 1$, the most probable value of g_m tends to zero. This is exactly what one would expect to happen in a resonance tunneling experiment at zero temperature: The conductance is maximum when the barriers are identical.

For the intermediate regime, when $\alpha_{1,2}\Delta \ll T \ll \Delta$, it is convenient to rescale the distribution to obtain[6]

$$\mathcal{R}_1(x) \equiv \frac{\sqrt{\alpha_1\alpha_2}\Delta}{4T} R_1(g_m) = x e^{-ax}[K_0(x) + aK_1(x)] \ , \tag{15}$$

where

$$x \equiv \frac{4Tg_m}{\sqrt{\alpha_1\alpha_2}\Delta} \ , \tag{16}$$

and $K_n(x)$ is the modified Bessel function of order n. Notice that the rescaling of g_m to x and of R_1 to $\mathcal{R}_1$ turned the distribution into a temperature-independent function, whose form depends only on the asymmetry between the leads. We also point out that for both temperature regimes, one has an finite offset in the distribution, i.e., $R_1(g_m \to 0) \neq 0$.

V. TWO-POINT LEADS

In the previous section we reviewed known results. In this and the following sections the main goal will be to study the effect of extended leads in the distribution of level widths and conductance peaks. We start by analyzing the situation of two-point leads, where the level width is given by

$$\gamma_i = \frac{\alpha_i \Delta}{\pi}(v_1 + v_2) \ . \tag{17}$$

The amplitudes are defined as $v_i = V|\psi_\nu(r_i)|^2$, $i = 1, 2$. When the points 1 and 2 are far apart ($r = |r_1 - r_2| \gg \lambda$), the amplitudes fluctuate independently and the distribution of level widths is equal to the convolution of the distributions for the isolated amplitudes [see Eq. (12)]. Consequently,

$$P_2(\gamma_i) = \left(\frac{\pi}{\alpha_i \Delta}\right)^2 \gamma_i \ \exp\left(-\frac{\pi \gamma_i}{\alpha_i \Delta}\right) \ . \tag{18}$$

Notice that the most probable value of γ_i is not zero, as for the one-point case, but $\alpha_i\Delta/\pi$. This fact by itself signals a strong qualitative change in the distribution. What happens, then, when we move the points closer together, so that $r \approx \lambda$? This question can only be fully answered if we know the joint probability distribution

$$Q_2(v_1, v_2; r) = \left\langle \delta\Big(v_1 - V|\psi_\nu(r_1)|^2\Big) \ \delta\Big(v_2 - V|\psi_\nu(r_2)|^2\Big) \right\rangle \ . \tag{19}$$

However, a simple analysis can be made before one starts seeking the exact form of $Q_2(v_1, v_2; r)$: Since there is no special reason for $Q_2(0, 0; r)$ to be singular if $r \neq 0$, we should have $P_2(\gamma_i \to 0) \propto \gamma_i$. On the other hand, $Q_2(0, 0; 0)$ is apparently singular in order to Eq. (12) hold true.

The exact calculation of $Q_2(v_1, v_2; r)$ can be performed by the supersymmetry method.[23] The result depends on the symmetry of the Hamiltonian; here we will consider only the case of broken time-reversal invariance (unitary ensemble), which yields

$$Q_2(v_1, v_2; r) = \frac{1}{1 - f(r)^2} \ \exp\left(-\frac{v_1 + v_2}{1 - f(r)^2}\right) \ I_0\left(\frac{2f(r)}{1 - f(r)^2}\sqrt{v_1 v_2}\right) \ , \tag{20}$$

where $f(r)$ is the Friedel-like function

$$\begin{aligned} f(r) &= \frac{1}{\nu}\int \frac{dp}{(2\pi)^d} \ e^{-ip\cdot r} \ \delta(p^2/2m - E) \\ &= \begin{cases} J_0(2\pi r/\lambda) & (d = 2) \\ (\lambda/2\pi r)\sin(2\pi r/\lambda) & (d = 3) \end{cases} , \end{aligned} \tag{21}$$

and $I_0(x)$ and $J_0(x)$ are Bessel functions of order zero. The exact expression for the two-point distribution of level widths can be readily calculated:

$$P_2(\gamma_i) = \int_0^\infty dv_1 \int_0^\infty dv_2 \; Q(v_1, v_2; r) \; \delta\Big(\gamma_i - (\alpha_i\Delta/\pi)(v_1 + v_2)\Big)$$
$$= \left[\frac{\pi}{\alpha_i \Delta f(r)}\right] \; \exp\left(-\frac{\pi\gamma_i}{\alpha_i\Delta[1 - f^(r)^2]}\right) \sinh\left(\frac{\pi\gamma_i f(r)}{\alpha_i\Delta[1 - f(r)^2]}\right) \; . \qquad (22)$$

The limit $r \gg \lambda$ (points placed far apart) can be easily extracted from Eq. (22) and it agrees with Eq. (18). For the opposite limit, $r = 0$, when the points coincide, one gets

$$P_2(\gamma_i) = \left(\frac{\pi}{2\alpha_i\Delta}\right) \exp\left(-\frac{\pi\gamma_i}{2\alpha_i\Delta}\right) \; , \qquad (23)$$

which is the distribution for a pointlike lead with a coupling constant twice as large, as we would expect.

The large fluctuation tail of the distribution tends to an exponential function, just as Eq. (12). The correlation between points, however, renormalizes the coupling constant α_i to $\alpha_i[1 + f(r)]$. Notice also the linear behavior at $\gamma_i \to 0$, *for any* $r \neq 0$, consistent with what we anticipated. The slope of the distribution at small widths becomes steeper as the distance between points decreases, but the qualitative aspect is rather independent of $f(r)$ and one can usually approximate $P_2(\gamma_i)$ by Eq. (18).

We stress that the main effect of point correlation within the lead is that the characteristic number of channels of a lead is not quite accurately given by the cross section divided by the electron wavelength. We can say that there is a crossover between single and double-channel behavior driven by the distance (correlation) between the points, i.e., by the parameter $f(r)$.

In Fig. 2 we show some distributions of level widths for two-site leads with different site separations obtained from our numerical simulation. One observes that the correlation between sites is small, even for $r = 1$ (in lattice units) and at the low energy portion of the spectrum (where λ is larger than at the middle of the spectrum). This effect, peculiar to the tight-binding model adopted here, can also be visualized in Fig. 3, where we have plotted the density autocorrelator as a function of site separation.

Given Eq. (22) we can proceed to evaluate $R_2(g_m)$. In analogy to the pointlike case, an analytical treatment is viable only for the two temperature regimes $T \ll \alpha_{1,2}\Delta$ and $\alpha_{1,2}\Delta \ll T \ll \Delta$; for T comparable to $\alpha_{1,2}\Delta$, one has to compute the distribution numerically and the dependence on the temperature cannot be rescaled out of the distribution. For simplicity, we will concentrate on the analytical results. We first present the expression we obtained for the resonance conductance distribution in the $T \ll \alpha_{1,2}\Delta$ regime:

$$R_2(g_m) = \frac{\theta(1 - g_m)}{4f(r)^2\sqrt{1 - g_m}} \left\{ \frac{[1 + f(r)^2][1 + (2 - g_m)(a^2 - 1)]}{[1 + g_m(a^2 - 1)]^2} \right.$$
$$\left. - \frac{[1 - f(r)^2][1 + (2 - g_m)(a_+^2 - 1)]}{2[1 + g_m(a_+^2 - 1)]^2} - \frac{[1 - f(r)^2][1 + (2 - g_m)(a_-^2 - 1)]}{2[1 + g_m(a_-^2 - 1)]^2} \right\} \; , \qquad (24)$$

where

$$a_\pm = (a \pm f(r)\sqrt{a^2 - 1})/\sqrt{1 - f(r)^2} \; , \qquad (25)$$

and $f(r)$ is defined in Eq. (21). In Fig. 4 we show $R_2(g_m)$ for different values of $f(r)$ and the asymmetry parameter a. Notice that the most probable value of g_m is maximum when the leads are symmetric, as we have argued in the previous section.

Clearly, by setting $r = 0$ in Eq. (24) we recover Eq. (13). In the opposite limit, $r \gg \lambda$, we can expand all terms to $O(f^2)$ and obtain

$$R_2(g_m) = \frac{3g_m\theta(1-g_m)\left\{[1+8a^2(a^2-1)] + 2g_m(a^2-1)(1-4a^2) + g_m^2(a^2-1)^2\right\}}{4\sqrt{1-g_m}\,[1+g_m(a^2-1)]^4} \ . \quad (26)$$

The distribution of conductance peaks in the regime $\alpha_{1,2}\Delta \ll T \ll \Delta$ can again be expressed as a universal, temperature independent function if one uses the rescaling shown in Eqs. (15) and (16). After some straightforward manipulation we obtain

$$\mathcal{R}_2(x) = \frac{x^2}{4f(r)^2}\sum_{p=0}^{3}(-1)^p e^{-a_p x_p}[K_0(x_p) + a_p K_1(x_p)] \ , \quad (27)$$

where $x_0 = x/[1+f(r)]$, $x_2 = x/[1-f(r)]$, $x_{1,3} = x/\sqrt{1-f(r)^2}$, $a_{0,2} = a$, $a_1 = a_+$, and $a_3 = a_-$. In Fig. 5 we have plotted $\mathcal{R}_2(x)$ for different values of $f(r)$ and a. When we set $r = 0$ in Eq. (27), we recover Eq. (15) with coupling constants twice as large. On the other hand, in the limit $r \gg \lambda$, one has, after an expansion to $O(f^2)$,

$$\mathcal{R}_2(x) = \frac{x^2 e^{-ax}}{2}\left[x(a^2+1)K_0(x) + (2ax + 2a^2 - 1)K_1(x)\right] \ . \quad (28)$$

In both temperature regimes, the most notable difference between $R_2(g_m)$ and $R_1(g_m)$ is in the small g_m behavior: $R_2(g_m \to 0)$ is linear in g_m *for any* $r \neq 0$, in contrast to $R_1(g_m)$, which tends to a constant in the same limit. Correlations between points within the leads do not affect the linear dependence.

VI. N-POINT LEADS

Some of the conclusions we have drawn for the two-point lead are straightforward to extend to the N-point case. For instance, let us call $Q_N(v_1, v_2, ..., v_N)$ the joint probability distribution of the amplitudes $v_k = V|\psi(r_k)|^2$ at N points. Then, since $Q_N(0, 0, ..., 0)$ is nonsingular for any arrangement where points do not coincide (i.e., when no two points are completely correlated), we *always* have $P_N(\gamma_i \to) \propto \gamma_i^{N-1}$.

Unfortunately, the supersymmetry technique becomes impractical to use in any derivation where $N > 2$. We do not know of any other method suitable for this task either. Therefore, in this section we will simply assume that the point fluctuations within the leads are completely independent, which is certainly correct for small enough values of γ_i or g_m. We will then derive expressions for $P_N(\gamma_i)$ and $R_N(g_m)$ and look at the numerical simulations to gain some insight about the general case, when correlations can be present.

If the amplitudes v_k fluctuate independently, we are allowed to convolute N distributions given by Eq. (12) to obtain the distribution of level widths for a N-point lead. In this way, we find that

$$P_N(\gamma_i) = \frac{1}{\Gamma(N)}\left(\frac{\pi}{\alpha_i\Delta}\right)^N \gamma_i^{N-1}\ \exp\left(-\frac{\pi\gamma_i}{\alpha_i\Delta}\right) \ , \quad (29)$$

where $\gamma_i = (\alpha_i \Delta/\pi) \sum_{k=1}^{N} v_k$, and, according to our definition, $\langle \gamma_i \rangle = N\alpha_i\Delta/\pi$. In the limit $N \gg 1$ one can check that the distribution becomes Gaussian around $\gamma_i \approx \alpha_i \Delta N/\pi$, with a width proportional to $1/\sqrt{N}$,

$$P_N(\gamma_i) \approx \frac{1}{\sqrt{2\pi N}} \left(\frac{\pi}{\alpha_i \Delta} \right) \exp\left(-\frac{(\gamma_i - \alpha \Delta N/\pi)^2}{2\alpha^2 \Delta^2 N/\pi^2} \right) . \tag{30}$$

The results of our simulations for N =4, 9 and 16 are shown in Fig. 6 for two different lead geometries and for extended eigenstates around the bottom of the energy band. The deviation from Eq. (30) becomes substantial for large N when the lead sites are close together. This indicates that the modest site-to-site correlation (see Fig. 3) can add up to make the effective number of channels smaller than the number of sites, particularly for small widths. As we move the sites farther apart, correlations become negligible and the distributions start to agree with Eq. (30).

From Eq. (29), together with Eqs. (6), (9), and (8), we can proceed to evaluate $R_N(g_m)$. In the very low temperature regime, $T \ll \alpha_{1,2}\Delta$, we obtain

$$R_N(g_m) = \frac{(g_m/4)^{N-1} \Gamma(2N)\ \theta(1-g_m)}{2\Gamma(N)\sqrt{1-g_m}[1+g_m(a^2-1)]^{2N}} \sum_{k=0}^{N} \frac{(2N)! a^{2(N-k)} [(a^2-1)(1-g_m)]^k}{(2N-2k)!(2N+2k)!}, \tag{31}$$

which contains all the essential features of R_1 and R_2. In the other regime, where $\alpha_{1,2}\Delta \ll T \ll \Delta$, we obtain, after an appropriate rescaling,

$$\mathcal{R}_N(x) = \left(\frac{x}{2} \right)^{2N-1} \frac{(2N)! e^{-ax}}{\Gamma(N)^2} \left\{ \frac{K_0(x)}{(N!)^2} + \sum_{l=1}^{N} \frac{[(\alpha_1/\alpha_2)^{l/2} + (\alpha_2/\alpha_1)^{l/2}] K_l(x)}{(N-l)!(N+l)!} \right\} . \tag{32}$$

One can easily check that Eq. (31) becomes equivalent to Eqs. (13) and (26) for $N = 1$ and $N = 2$, respectively. Similarly, Eq. (32) is reduced to Eq. (15) for $N = 1$, and to Eq. (28) for $N = 2$. We remark that both Eqs. (31) and (32) yield the same limit $R_N(g_m \to 0) \propto g_m^{N-1}$, i.e., the distributions behave like a power law for small peak heights.

The large N limit makes the distribution of conductance peaks narrower. For instance, when $N \gg 1$, Eq. (32) tends to a Gaussian law, centered around $x \sim O(N)$,

$$\mathcal{R}_N(x) \approx \frac{a}{\sqrt{4\pi N}} \exp\left(-\frac{(x - 2N/a)^2}{4N/a^2} \right) . \tag{33}$$

Because $\langle g_m \rangle \sim O(N)$, but $\delta g_m \sim O(\sqrt{N})$, fluctuations in the height of resonance peaks are suppressed for very large leads. This should be contrasted to the universal fluctuations of conductance as a whole, which obey $\langle g_m \rangle / \delta g_m \sim O(1)$. Furthermore, $\langle g_m \rangle \propto (1/\alpha_1 + 1/\alpha_2)^{-1}$, which is the classical result (Ohm's law).

VII. CONCLUSIONS

We have considered the statistics of the widths of electronic states inside a quantum dot coupled to a bulk reservoir through contact leads. It is well-known that in the case of

pointlike contacts the distribution of widths obeys a universal exponential law, which corresponds to Gaussian fluctuations of the wavefunction. We have shown that the statistics of the widths is strongly influenced by the size of the contact area between the leads and the dot. For two-point contacts we presented the exact expression for the distribution function of widths and found that it closely resembles the result one obtains by assuming no correlation between the points. The correlation effects appear only for large fluctuations, whose contribution to any observable quantity is exponentially small. Following this observation, we suggested that the N-point lead can be considered as a set of N points fluctuating independently. We evaluated the distribution of widths analytically and compared the results with direct measurements from numerical simulations. A good qualitative agreement was found.

The central region of the distribution tends to be Gaussian as N increases. Therefore, the fluctuations in the level width are suppressed for large leads and we can describe the dot in terms of the average parameters. In the region of very large widths, the distribution does not follow a Gaussian law, but rather decays exponentially. For small widths, the distribution behaves as a power law.

For the continuous system with extended leads we can expect a similar behavior. The distribution of widths is Gaussian around the average, which is proportional to the effective number of channels $N_0 = A/\lambda^{d-1}$, where A is the cross section of the lead contact. The tail of the distribution for very large widths is exponential. In the region of small widths the distribution behaves as

$$P(\gamma_i) \propto \gamma_i^N \ . \tag{34}$$

The effective number of channels N is equal to the number of independent "points" in the lead, which increases for small γ_i as $N \propto N_0/\gamma_i$.

The relevance of these results to experiments appears in the determination of the distribution of conductance peaks in the resonance regime. The main consequence of the finite extension of the leads is found in the power law behavior of the distribution at small peak heights. As the lead becomes very large, the distribution tends to a Gaussian law. The possibility of asymmetry between the leads is taken into account in our work. Finally, we point out that Eqs. (24) and (27) can be used to describe the statistics of four-probe dots where the constrictions are made very narrow (pointlike leads).

Acknowledgments

We would like to thank A. Andreev, M. Faas, K. Efetov, C. Lewenkopf, C. Marcus, and B. Simons for useful discussions. E. R. M. acknowledges the financial support of Conselho Nacional de Desenvolvimento Científico e Tecnológico (CNPq, Brazil). This work was supported through a NSF Grant No. DMR 92-04480.

REFERENCES

[1] *Nanostructures and Mesoscopic Systems*, edited by W. P. Kirk and M. A. Reed (Academic Press, San Diego, 1992).

[2] M. A. Kastner, Rev. Mod. Phys. **64**, 849 (1992).

[3] *Single Charge Tunneling*, edited by H. Grabert and M. Devoret (Plenum Press, New York, 1992).

[4] R. Landauer, IBM J. Res. Dev. **1**, 223 (1957); Philos. Mag. **21**, 863 (1970).

[5] M. Büttiker, Phys. Rev. Lett. **57**, 1761 (1986); IBM J. Res. Dev. **32**, 317 (1988).

[6] V. N. Prigodin, K. B. Efetov, and S. Iida, Phys. Rev. Lett. **71**, 1230 (1993).

[7] H. U. Baranger and P. A. Mello (unpublished).

[8] R. A. Jalabert, J.-L. Pichard, and C. W. J. Beenakker (unpublished).

[9] R. A. Jalabert, A. D. Stone, Y. Alhassid, Phys. Rev. Lett. **68**, 3468 (1992).

[10] A. D. Stone and H. Bruus, Physica B **189**, 43 (1993); Surf. Sci. **305**, 490 (1994).

[11] K. B. Efetov, Adv. Phys. **32**, 53 (1983).

[12] J. J. M. Verbaarschot, H. A. Weidenmüller, and M. R. Zirnbauer, Phys. Rep. **129**, 367 (1985).

[13] H. U. Baranger, R. A. Jalabert, and A. D. Stone, Chaos **3**, 665 (1993).

[14] C. M. Marcus, R. M. Westervelt, P. F. Hopkins, and A. C. Gossard, Phys. Rev. B **48**, 2460 (1993); Chaos **3**, 643 (1993); Surf. Sci. **305**, 480 (1994).

[15] D. Weiss, K. Richter, A. Menschig, R. Bergmann, H. Schweizer, K. von Klitzing, and G. Weimann, Phys. Rev. Lett. **70**, 4118 (1993).

[16] M. J. Berry, J. A. Katine, C. M. Marcus, R. M. Westervelt, and A. C. Gossard, Surf. Sci. **305**, 480 (1994).

[17] M. W. Keller, O. Millo, A. Mittal, D. E. Prober, and R. N. Sacks, Surf. Sci. **305**, 501 (1994).

[18] T. M. Fromhold, M. L. Leadbeater, L. Eaves, T. J. Foster, P. C. Main, and F. W. Sheard, Surf. Sci. **305**, 511 (1994).

[19] S. Tomsovic and E. J. Heller, Phys. Rev. Lett. **70**, 1405 (1993).

[20] M. R. Zirnbauer, Phys. Rev. Lett. **69**, 1584 (1992).

[21] N. Taniguchi, A. Hashimoto, B. D. Simons, and B. L. Altshuler, Europhys. Lett. (to be published).

[22] M. V. Berry, in *Chaos and Quantum Physics*, edited by M.-J. Giannoni, A. Voros, and J. Zinn-Justin (North-Holland, Amsterdam, 1991), p. 251; Philos. Trans. R. Soc. London **A237**, 237 (1977).

[23] V. N. Prigodin (unpublished).

FIGURES

FIG. 1. Histogram of level widths for single-site leads at two regions of the energy band: middle (circles) and bottom (squares). The dashed line is the universal prediction (exponential law). The level width is rescaled so that $\langle\gamma_i\rangle = 1$.

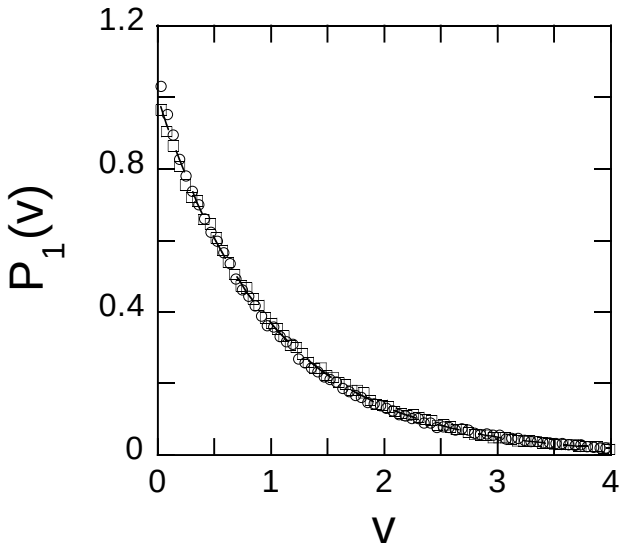
FIG. 2. Histograms of level widths for two-site leads at two regions of the energy band: middle (squares) and bottom (circles). The level width is rescaled so that $\langle\gamma_i\rangle = 2$. r is the distance in lattice units between sites within the lead. The solid and dashed curves are the predictions for $f(r)$=0.35 and $f(r) = 0$, respectively.

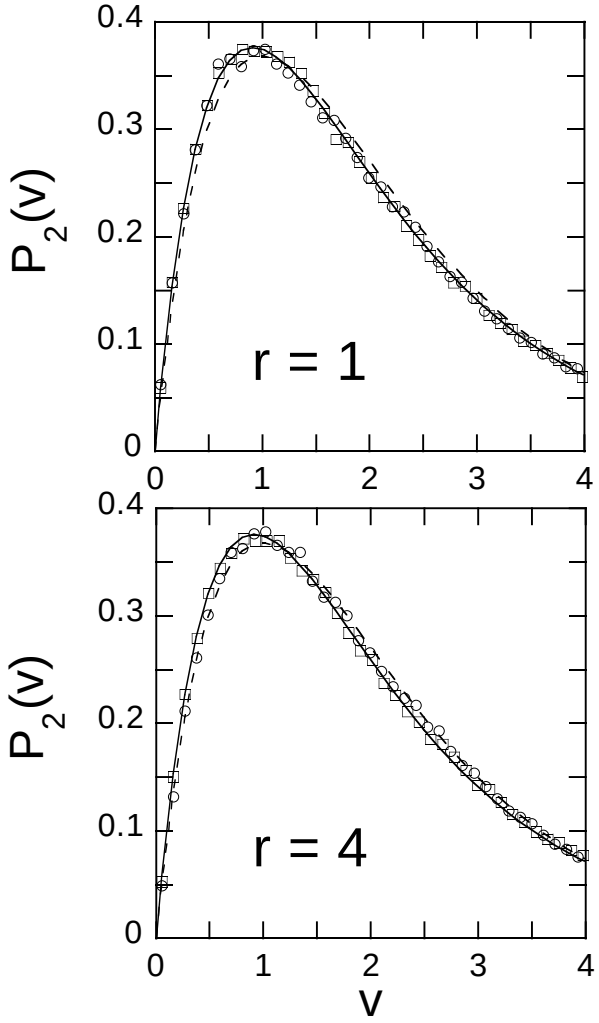
FIG. 3. Density-density correlator as a function of site separation for two regions of the energy band: middle (circles) and bottom (squares). The density is defined as $\rho(r) = |\psi_\nu(r)|^2$ and the average is performed over ν (eigenstate) and grid location.

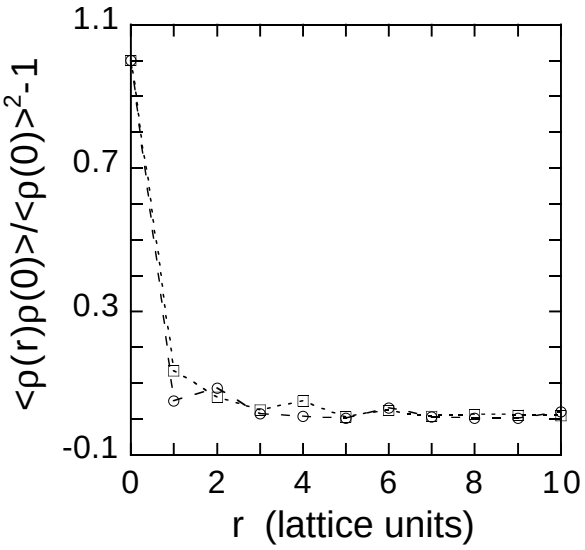
FIG. 4. Distribution of resonance conductance peaks in a dot with two-point leads at very low temperatures ($T \ll \alpha_{1,2}\Delta$). The main plot shows the curves for the symmetric case (a=1) and different separation of lead sites. Notice the liner behavior as $g_m \to 0$ for any f$\neq$1. The insert shows the dependence with the asymmetry parameter for a fixed distance between sites (f=0.5).

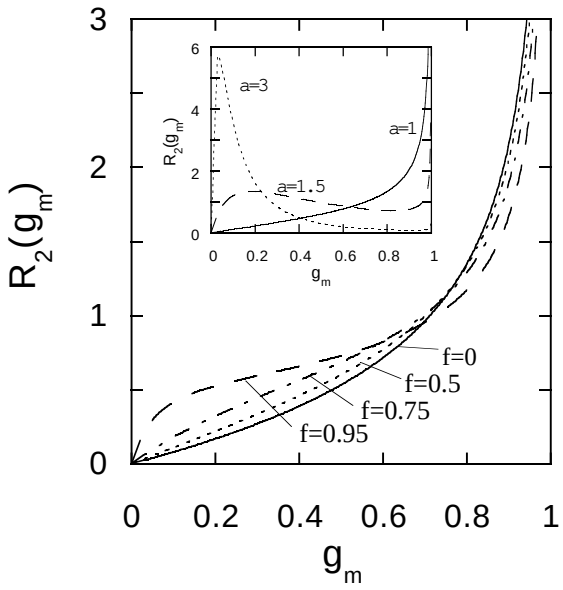
FIG. 5. Distribution of resonance conductance peaks in a dot with two-point leads at intermediate temperatures ($\alpha_{1,2}\Delta \ll T \ll \Delta$). The conductance is expressed in the rescaled form $x = 4Tg_m/\sqrt{\alpha_1\alpha_2}\Delta$. The main plot shows the curves at a=1 (symmetric case) and variable distance between the lead sites. The insert shows the dependence on the asymmetry parameter for a fixed f=0.5.

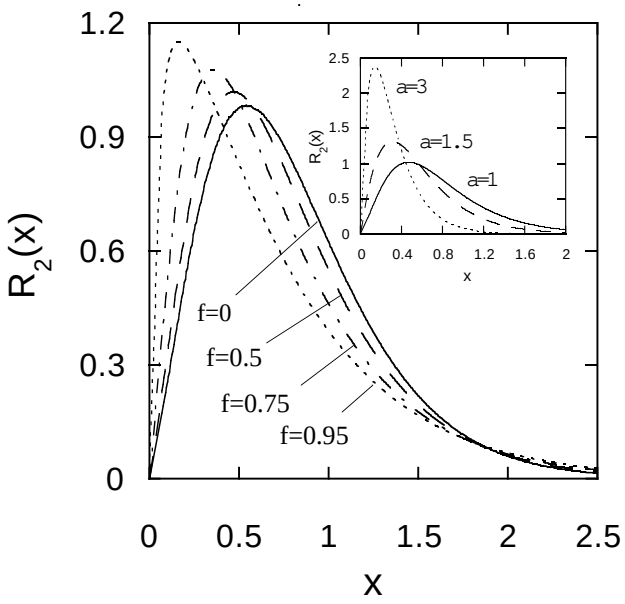
FIG. 6. Histogram of level widths for N-site leads and for eigenstates at the bottom of the energy band. The level width is rescaled so that $\langle\gamma_i\rangle = N$. The dashed line is the prediction for independent site fluctuations of the wavefunction. The squares correspond to leads where sites were placed together ($r = 1$) and the circles correspond to leads with $r = 3$. As an example, in the insert we show how a N=4 lead with $r = 2$ was implemented.

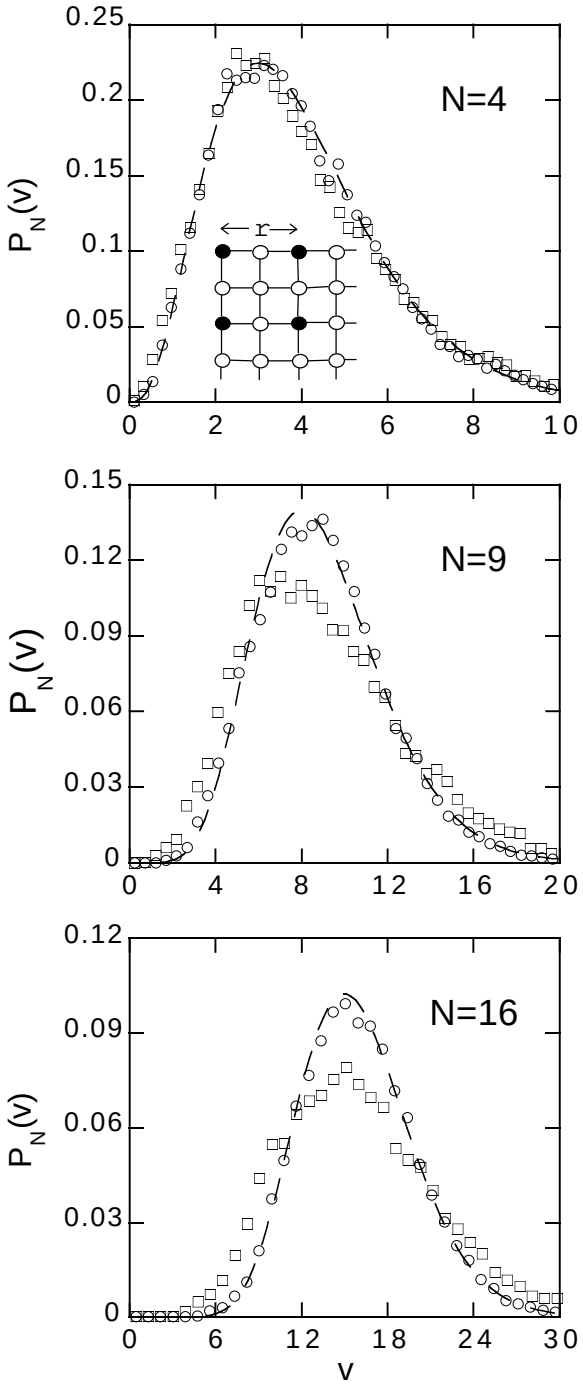

1.2
0.8
0.4
0
0
1
2
3
4
V
P1(v)


0.4
0.3
0.2
0.1
0
$P_2(v)$
r = 1
0
1
2
3
4
0.4
0.3
0.2
0.1
0
$P_2(v)$
r = 4
0
1
2
3
4
v


1.1
0.7
0.3
-0.1
0
2
4
6
8
10
r (lattice units)
<ρ(r)ρ(0)>/<ρ(0)>2-1


3
2
1
0
0
0.2
0.4
0.6
0.8
1
$R_2(g_m)$
g_m
f=0
f=0.5
f=0.75
f=0.95
6
4
2
0
a=3
a=1
a=1.5
$R_2(g_m)$
g_m


1.2
0.9
0.6
0.3
0
0
0.5
1
1.5
2
2.5
x
R2(x)
f=0
f=0.5
f=0.75
f=0.95
a=3
a=1.5
a=1
R2(x)
x


N=4
N=9
N=16
$P_N(v)$
v
r
0.25
0.2
0.15
0.1
0.05
0
0.12
0.09
0.06
0.03
0
2
4
6
8
10
12
16
18
20
24
30